

Supporting Information for:

Methylene Blue Exciton States Steer Nonradiative Relaxation: Ultrafast Spectroscopy of Methylene Blue Dimer

Jacob C. Dean, Daniel G. Oblinsky, Shah Nawaz Rafiq, and Gregory D. Scholes^{*}

Department of Chemistry, Princeton University, Princeton, New Jersey 08544

1. TG-FROG map of NOPA pulse	p. S2
2. Time-resolved fluorescence of MB	p. S2
3. MB pump-probe anisotropy decay	p. S3
4. Coherent oscillations of MB and MB₂ in broadband transient absorption	p. S5
5. Diagonal and anti-diagonal line-widths of MB and MB₂	p. S6
6. Two-dimensional oscillation maps of sample 2 (high concentration)	p. S7
7. Decay-associated spectra (DAS) of MB and MB₂	p. S9

1. TG-FROG map of NOPA pulse

The TG-FROG map of the pulse used in the 2DES experiments is shown in Figure S1.

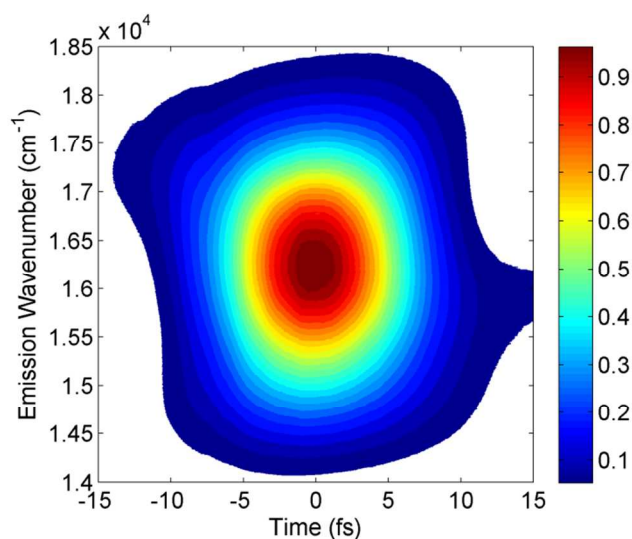


Figure S1. TG-FROG map of NOPA pulse used in 2DES experiment.

2. Time-resolved fluorescence of MB

The fluorescence decay of MB following excitation at $\lambda = 653$ nm is shown in Figure S2. The fit was performed using a single exponential with re-convolution analysis to properly account for the instrument response function of the system. The data is an average of five independent measurements yielding a time constant of $\tau_F = 370 \pm 1$ ps.

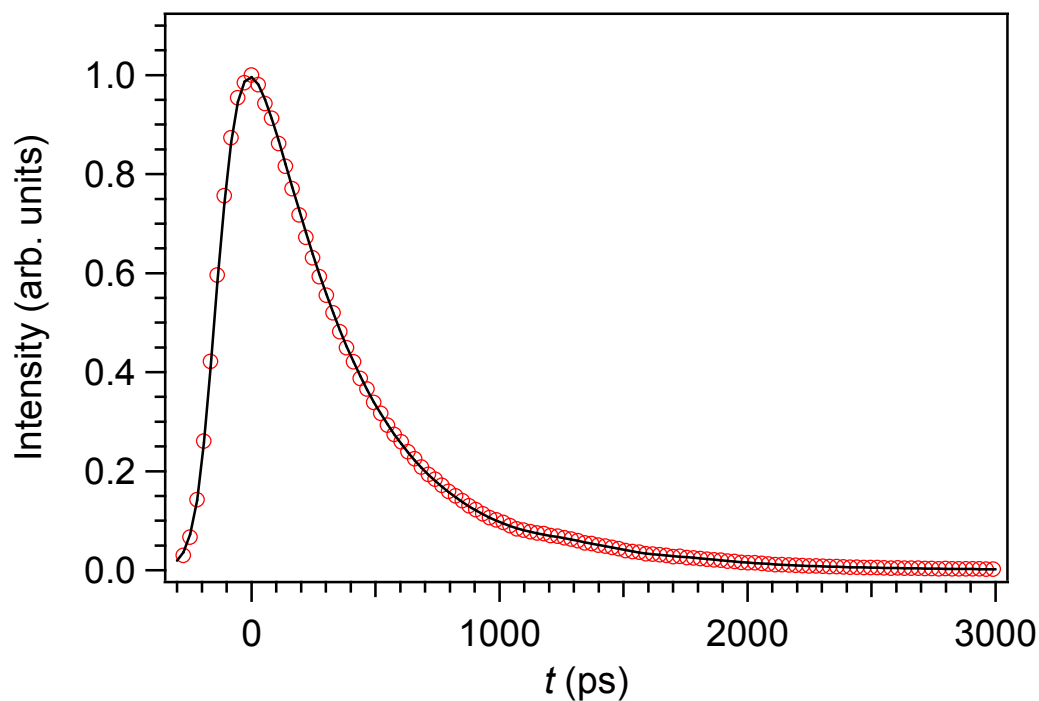


Figure S2. Time-correlated single photon counting fluorescence decay of MB (red) with fit.

3. MB pump-probe anisotropy decay

The anisotropy of pump-probe signals is a measure of the reorientation of the transition dipole moment (TDM), initially prepared by the leading pump pulse, as a function of delay time. This process can occur as a result of electronic energy transfer from an initially excited donor to an acceptor, or more relevant to this case, it is also a measure of the rotational reorientation of the chromophore in solution. The anisotropy is calculated from two pump-probe measurements with different polarization conditions between pump and probe beams: parallel, S_{\parallel} , and perpendicular, S_{\perp} . The anisotropy was then calculated by:

$$r = \frac{S_p - S_{\perp}}{S_p + 2S_{\perp}} \quad (\text{S1})$$

The values of r range from 0.4 to -0.2 in the limits of no reorientation (unaltered alignment of TDM) and rotation of the vector perpendicular to the original TDM axis (defined by the pump) respectively. The anisotropy decay of the monomer near the peak of the BBTA signal ($\sim 15000 \text{ cm}^{-1}$) is shown in Figure S3. The anisotropy decay can be fit with a single exponential with a constant offset (approximation of longer decay), and the fit was applied to points after $\Delta t = 0.08 \text{ ps}$ to avoid the coherent artifact. The fit yields a time constant of $\tau_{\text{an}} = 116 \pm 6 \text{ ps}$ (2σ). As expected for a molecule of this size, the anisotropy begins at ~ 0.4 and decays very near to 0.0 indicating the loss of a well-defined polarization relationship between TDM and pump. This loss of “memory” is due to rotational diffusion of MB following excitation.

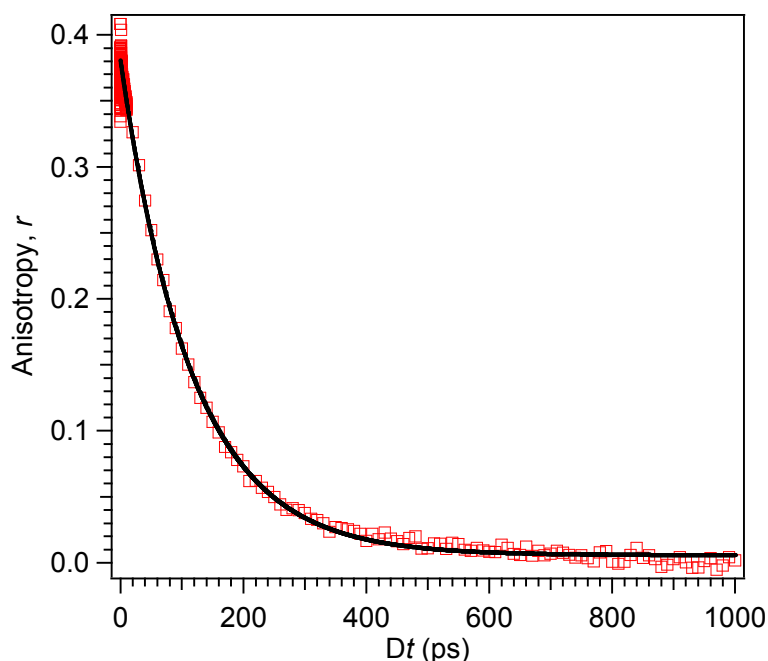


Figure S3. Anisotropy decay (red) and fit (black) of MB BBTA taken at 15000 cm^{-1} .

4. Coherent oscillations of MB and MB₂ in broadband transient absorption

The vibrational coherences present in MB have been discussed and assigned in detail in Dean *et al.*¹ The coherent dynamics of sample 2 in the current work, which incorporates a large concentration of MB₂, were given in Figure 5 of Section 3.B., and a brief description can be found there. Figure S4a shows traces taken from the coherent BBTA spectrum in Figure 5b along with their corresponding Fourier transform spectra (Figure S4b). Sample 2 traces and spectra are given in black, while the pure MB sample 1 is shown for comparison in red. Very little difference exists between samples 1 and 2, demonstrating that most of the coherent amplitude is due to MB monomer. While the amplitude is necessarily smaller in the MB GSB/SE region of the BBTA spectrum at lower wavenumber in sample 2, higher emission wavenumber near the MB₂ GSB does give some differences in relative amplitude. In particular, the 450 cm⁻¹ ring mode fundamental is larger than the neighboring 500 cm⁻¹ band. Also, the 770 cm⁻¹ fundamental still appears with modest amplitude, while a reduction in the overtone at 860 cm⁻¹ is clear. This reduction is a result of the decrease in Franck-Condon factors as a consequence of delocalization/exchange narrowing.

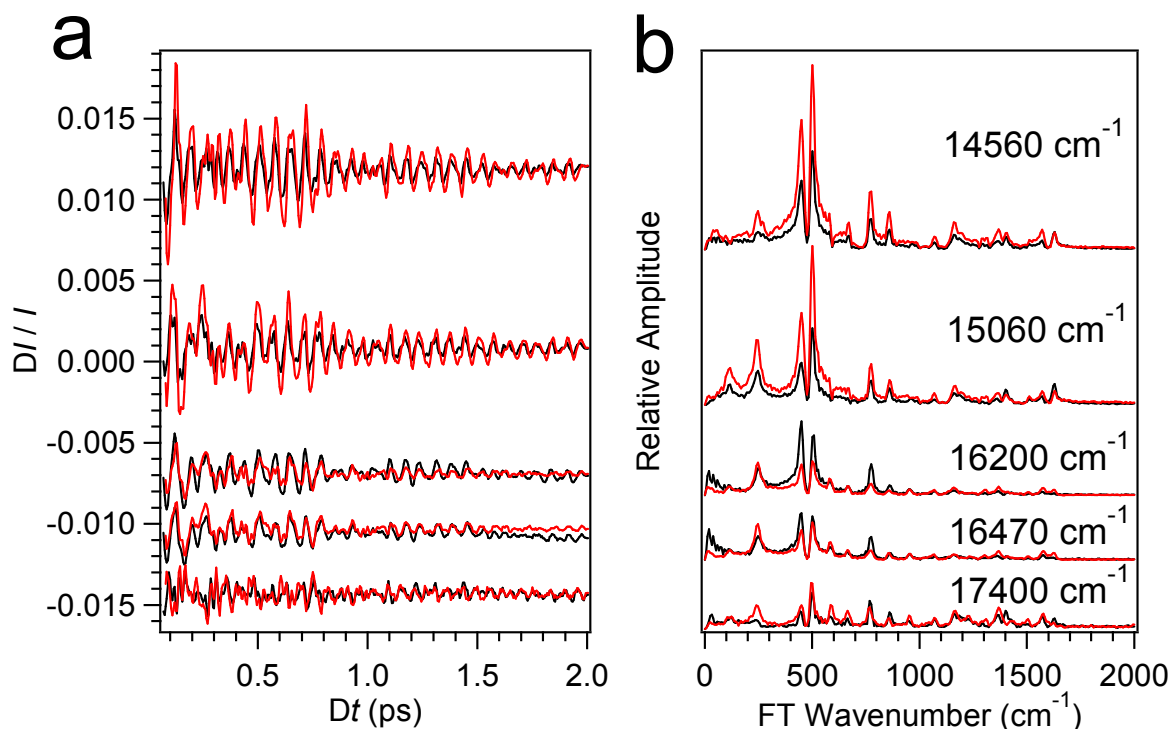


Figure S4. (a) Traces of coherent BBTA and (b) corresponding FT spectra for sample 1 (red) and sample 2 (black) at various emission wavenumbers.

5. Diagonal and anti-diagonal line-widths of MB and MB₂

The lineshape analysis of MB and MB₂ 2D peaks revealed drastically different behavior at 298 K and 77 K leading to the conclusion that the MB₂ homogeneous linewidth is limited by the lifetime of the S₊ state. This discussion is given in detail in Sections 3.C. and 4.B., and the diagonal/anti-diagonal linewidth ratio's are given in Figure 7c and 8d. The individual diagonal (solid line, squares) and anti-diagonal linewidths (dotted line, circles) making up the reported ratios are reported in Figure S5. MB is displayed in red, while MB₂ is shown in black. As discussed in the text, the anti-diagonal width of MB is significantly reduced in going from 298 K to 77 K ($\sim 1200 \rightarrow 600$ cm⁻¹), while MB₂ changes only slightly from $\sim 1100 \rightarrow 850$ cm⁻¹.

Alternatively, the diagonal width of the monomer remains constant between both temperatures as expected when the diagonal linewidth is dominated by inhomogeneous broadening, while MB₂ is reduced by a similar amount as its anti-diagonal. It is noted however that the value of D/AD is a better comparator as it is less sensitive to spectral filtering along the diagonal which can occur due to the limited bandwidth of the NOPA pulses used.²

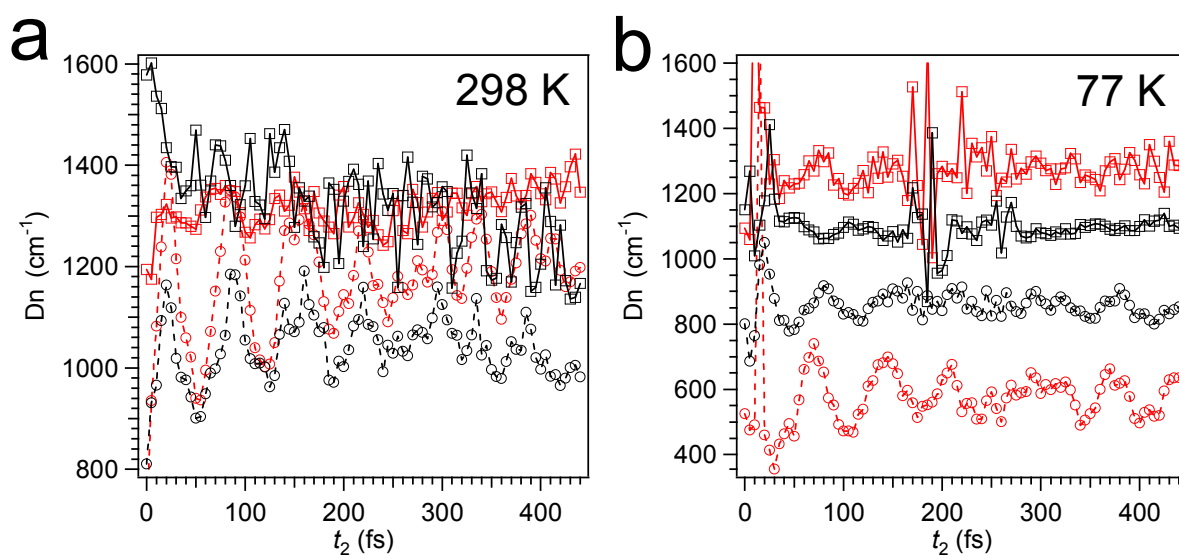


Figure S5. Diagonal (solid lines, squares) and anti-diagonal (dotted lines, circles) linewidths of MB (red) and MB₂ (black) at (a) 298 K and (b) 77 K.

6. Two-dimensional oscillation maps of sample 2 (high concentration)

The coherent BBTA and 2DES of sample 2 revealed that vibrational coherences in MB₂ were significantly less active than MB, particularly when weighted against the total signal amplitude. The comparison of FT spectra in Figure S4 shows that the frequencies of the most vibronically-active coherences are identical between monomer and dimer, with only minor changes in relative amplitude. To disperse this Fourier amplitude into two-dimensions, 2D

oscillation maps were generated for sample 2 by Fourier transformation of the full 2DES data set along t_2 (every ν_1, ν_3 point) after subtracting out the population dynamics. This analysis was used in the case of MB for aiding assignments of the coherences observed in BBTA, resulting in signatures for combination bands and overtones.¹ Here, we show the oscillation maps for sample 2 to isolate coherences in the 2D spectra to MB₂. This data is shown in Figure S6 at various ν_2 , or FT frequencies.

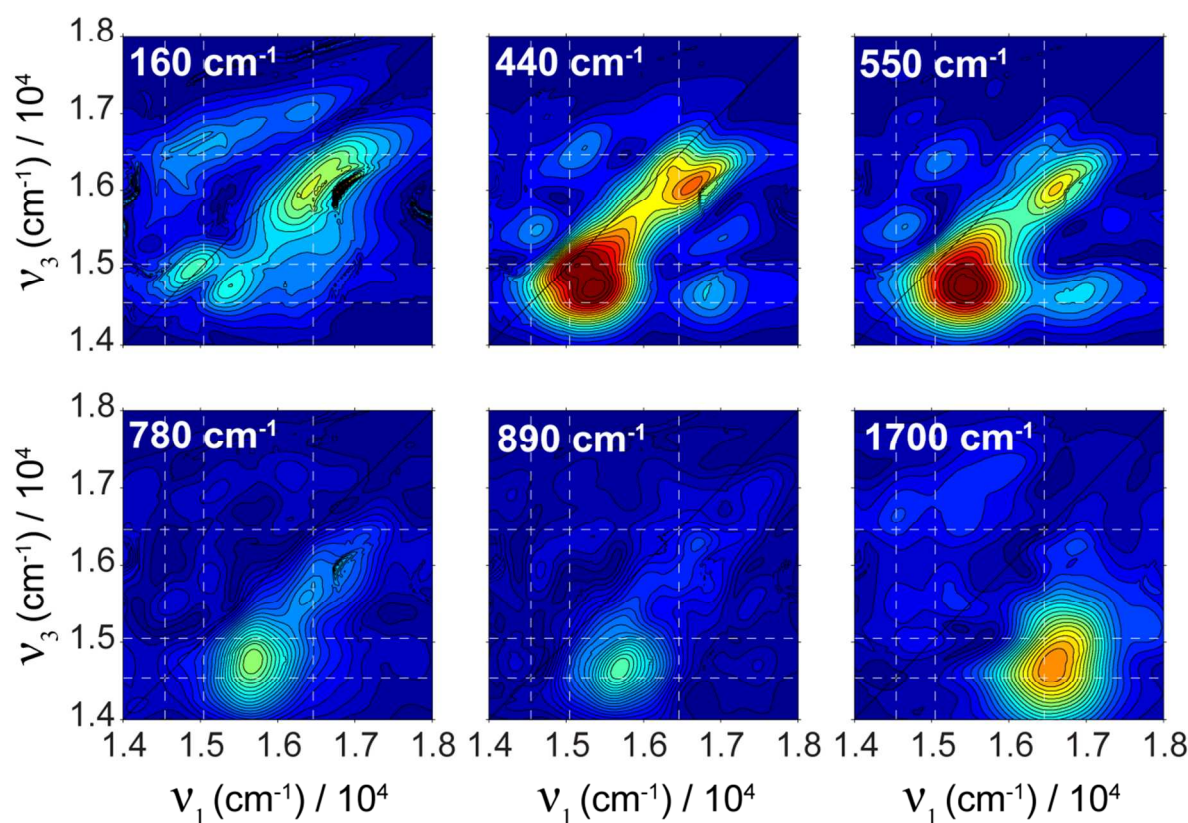


Figure S6. 2D oscillation maps of sample 2 at various ν_2 frequencies.

Given the limited t_2 range of 440 fs in the 2DES experiment, the ν_2 frequency resolution is lower than BBTA resulting in slightly different reported frequencies for some coherences. The

two largest coherences, $\nu_2 = 440$ and 550 cm^{-1} assigned to the central ring mode fundamentals display large amplitude below the MB diagonal position in agreement with the previous assignment to predominantly ground state coherence. Additionally, now amplitude arises in the same position below the MB₂ diagonal signaling the same assignment. The higher frequency coherences are nearly identical to those taken from sample 1, signifying their assignment to MB. These data further support the former conclusion that vibronic excitations are less present in MB₂, providing further evidence that the source of line broadening observed in the experiment is related predominantly to lifetime considerations and not to bath interactions.

7. Decay-associated spectra (DAS) of MB and MB₂

Global analysis was initially performed on both sample 1 and sample 2 transient absorption data for estimating the number of components and their associated decay rates to be included in target analysis as initial parameters. After fitting the data with the appropriate model represented in Figures 9 and 10 in Section 4.A., the decay-associated spectra (DAS) were extracted and are shown in Figures S7 and S8. The time constants affiliated with each DAS are given in Figures 9 and 10 for the corresponding SAS.

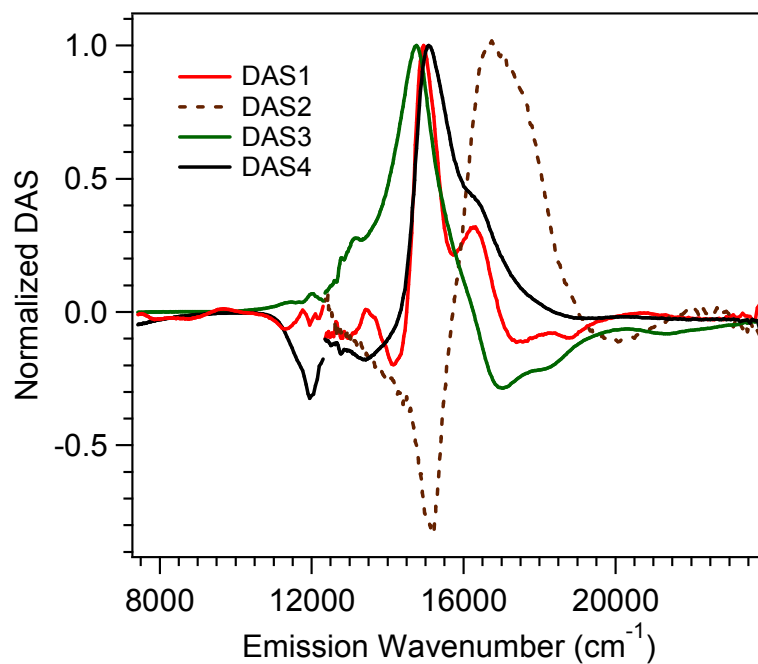


Figure S7. Decay-associated spectra for sample 1 transient absorption.

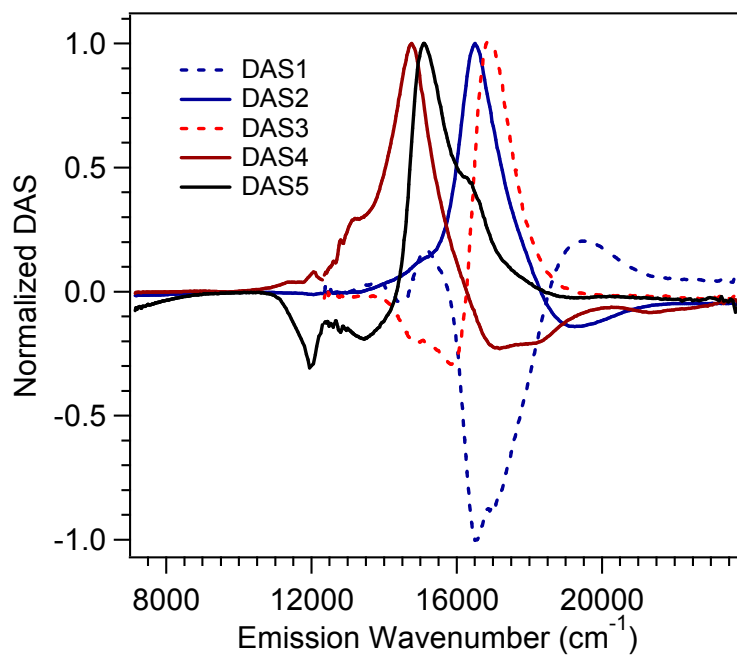


Figure S8. Decay-associated spectra for sample 2 transient absorption.

References

- (1) Dean, J. C.; Rafiq, S.; Oblinsky, D. G.; Cassette, E.; Jumper, C. C.; Scholes, G. D. Broadband Transient Absorption and Two-Dimensional Electronic Spectroscopy of Methylene Blue. *J. Phys. Chem. A* **2015**, *119*, 9098-9108.
- (2) Nemeth, A.; Lukes, V.; Sperling, J.; Milota, F.; Kauffmann, H. F.; Mancal, T. Two-Dimensional Electronic Spectra of an Aggregating Dye: Simultaneous Measurement of Monomeric and Dimeric Line-Shapes. *Phys. Chem. Chem. Phys.* **2009**, *11*, 5986-5997.